


The fabrication of 3D surface scaffold of collagen/poly (L-lactide-co-caprolactone) with dynamic liquid system and its application in urinary incontinence treatment as a tissue engineered sub-urethral sling: In vitro and in vivo study

Kaile Zhang MD, PhD¹ | Nailong Cao MD¹  | Xuran Guo MD² |
Qingsong Zou MD¹ | Shukui Zhou PhD¹ | Ranxing Yang MD¹ |
Weixin Zhao MD³ | Xiumei Mo PhD² | Wei Liu PhD⁴ | Qiang Fu MD, PhD¹

¹ The Department of Urology, Affiliated Sixth People's Hospital, Shanghai Jiaotong University, Shanghai, China

² Biomaterials and Tissue Engineering Laboratory, College of Chemistry & Chemical Engineering and Biotechnology, Donghua University, Shanghai, China

³ Wake Forest Institute for Regenerative Medicine, Winston-Salem, North Carolina

⁴ Trauma Department of Orthopedics, Shenzhen Second People's Hospital, Shenzhen, China

Correspondence

Qiang Fu, The Department of Urology, Affiliated Sixth People's Hospital, Shanghai Jiaotong University, Shanghai, China.
Email: jamesqfu@aliyun.com

Xiumei Mo, Biomaterials and Tissue Engineering Laboratory, College of Chemistry & Chemical Engineering and Biotechnology, Donghua University, Shanghai, 201620, China.
Email: xmm@dhu.edu.cn

Funding information

Science and Technology Commission of Shanghai Municipality, Grant number: 14JC1492100

Aims: To fabricate a novel nanoyarn biomaterial via a dynamic liquid electrospinning system, and to simultaneously evaluate whether nanoyarn is capable of being applied as a urinary sling for future clinical transfer.

Methods: Nanoyarn was cultured with adipose-derived stem cells (ADSCs). Cell morphology and function were observed on nanoyarn. Female rats that underwent vagina dilatation (VD) and bilateral ovarian resection (BOR) were used as the urinary incontinence model. After 2 weeks, the cells-sling was fixed to the suburethra. A commercial sling that tension-free vaginal tape-obturator (TVT-O) was used as a control. The urodynamic test for leak point pressure (LPP) and histological tests were used to evaluate the sling's performance in vivo.

Results: The nanoyarn possessed beneficial properties and the actin filament from ADSCs, which is very similar to muscle. Rats that underwent VD and BOR maintained a low LPP, whereas the LPP in rats with VD alone recovered to normal levels within 2 weeks. LPP in the nanoyarn group gradually decreased on the three urodynamic tests post-suburethral surgery, however, the cell-laden nanoyarn maintained LPP at normal levels for 8 weeks; the TVT-O group showed a significant increase in LPP at 8 weeks. Cell-laden nanoyarn was infiltrated with more cells, collagen, and vessels than the controls.

Conclusions: The nanoyarn showed sufficient efficacy to maintain LPP in urinary incontinence rat model. In addition, it improved cell infiltration, collagen and muscle development compared to TVT-O. Thus, the combination of ADSCs and a nanoyarn scaffold could be a promising tissue-engineered sling for the treatment of urinary incontinence.

KEYWORDS

dynamic liquid system, electrospinning, suburethral sling, tissue engineering, urinary incontinence

Limin Liao led the peer-review process as the Associate Editor responsible for the paper.

Kaile Zhang and Nailong Cao contributed equally to this work.

1 | INTRODUCTION

Urinary incontinence (UI) affects the life quality of women worldwide.¹ Implanting a suburethral sling to elevate leak point pressure (LPP) has become a choice for women suffering from this disease.² About 10-20% of women developed recurrent incontinence according to data from a commercial sling implantation clinic.³ Furthermore, complications associated with implanting a sling, including sling erosion, obstructive voiding, and persistent pain, are frequently reported.⁴ In this study, we tested a novel tissue engineered sling consisting of a biomaterial and stem cells to reinforce the efficacy and decrease complications after sling surgery.

The purpose of tissue engineering and regenerative medicine is to use biomaterials with cells or cytokines to regenerate tissues similar to their natural counterparts.⁵ In this regard, electrospinning is a popular way to produce biomaterials for tissue engineering when suitable polymers are used. However, scaffolds fabricated with a normal electrospinning system possessed very low pore size, and the nutrients and waste of cells were not able to be exchanged throughout the scaffolds.⁶ Here, we applied a dynamic liquid electrospinning system to fabricate a biomimetic electrospun scaffold with a dynamic liquid electrospinning device. This scaffold, which is named nanoyarn, possessed aligned microstructures, larger pores, and high porosity. Furthermore, the nanoyarn was composed of type 1 collagen and poly (L-lactide-co-caprolactone) [P(LLA-CL)], which morphologically and structurally mimic the extracellular matrix (ECM) of native muscle tissue, especially for the triple helix structure of collagen. The nanoyarn scaffolds were seeded with adipose-derived stem cells (ADSCs), which possess highly efficient stemness and a minimally invasive procedure to harvest. In our previous study, the morphology and characteristics of nanoyarn and normal non-woven nanofibrous scaffolds were tested and compared *in vitro*.⁷ In this study, we extended the research to *in vivo* models, by evaluating the efficacy, safety, and tissue development of nanoyarn as a suburethral sling in a rat model.

2 | METHODS

The materials were previously reported.⁷ Briefly, P (LLA-CL) (LA: CL = 50:50, Mw = 300 000) was provided by Nara medical university (Shijocho, Japan). Type I collagen was obtained from Sichuan Ming-Rang Bio-Tech Co. Ltd. And Hexafluoroisopropanol (HFIP) was from Fine Chemicals, (Shanghai, China). The animals used in this study were approved by the ethical committee of Shanghai Sixth People's Hospital.

2.1 | Nanoyarn fabrication with a dynamic liquid system

The method for fabricating nanoyarn was previously reported.⁷ Briefly, a dynamic liquid supporting system and electrospinning equipment were used to fabricate the nanoyarn scaffolds. A hole (8 mm in diameter) was created in a basin (40 cm in diameter, 20 cm in depth), so it allows the flow of water to form a water vortex. A pump was employed to recycle the water back to maintain the water level after the water was drained through the hole into a tank below the basin. P (LLA-CL) and collagen was dissolved in HFIP, yielding a 50:50 blended solution (8 w/v %). The blended solution jet was located 15 cm above the water vortex, and the spinning rate was 1.0 mL/h under a high voltage of 15 kV. As the HFIP evaporated, electrospun nanofibers were generated and deposited on the water surface, and then the nanofibers were twisted into a bundle of nanoyarn in the water vortex and collected by a 5 cm-diameter rotating mandrel (60 r/min) to form the nanoyarn scaffold. Electrospun nanofibrous scaffolds were fabricated as control group to compare the morphology and cell infiltration with nanoyarn. The water and air temperature was room temperature which was set and maintained at 25°C by air conditioner.

2.2 | ADSCs harvesting

The ADSCs were harvested from the fat tissue of female rats and cultured in low glucose Dulbecco's Modified Eagle's Medium with 5% serum. After passage 2, the ADSCs were induced according to a previous protocol. Cell growth and morphology were constantly monitored by inverted microscopy.⁸

2.3 | Scanning electron microscopy

The dimension of the whole scaffold after electrospinning was nearly 160 mm × 60 mm × 0.5 mm. The scaffold samples were punched into 12 mm and examined by scanning electron microscopy (SEM). Then they were sterilized with ultraviolet light for 2 h and put in 24-well plates. Ten thousand cells in 1 mL complete medium were seeded onto the scaffolds. On day 1, 4, and 7, samples of scaffolds were washed with PBS to remove the non-adherent cells. Then the cells with scaffolds were fixed in 2.5% glutaraldehyde for 30 min at room temperature. Afterwards, they were dehydrated through a series of graded alcohol solutions. The drying process was conducted with the critical point dryer. The scaffolds were sputter coated with gold-palladium, and examined under SEM at 12 KV (Tescan Vega, Warrendale, PA).

2.4 | Scaffold porosity

A Vernier caliper was used to measure the exact size and volume (V) of the scaffolds. The side length and thickness

were measured, and the approximate volume was calculated. The dry scaffolds were weighed (W_d), submerged in absolute ethanol (r in density) for 2 h, and weighed again (W_s). The porosity was calculated as $(W_s - W_d)/r/V$, ($n = 3$).

2.5 | Pore size

The pore sizes of the nanoyarn and nanofiber scaffolds were measured with SEM images. Each pore of the nanoyarn and nanofiber scaffold was surrounded and a rhomboid or triangle was formed by the yarn, so the lengths of sides in the triangle and rhomboid were measured and recorded in Microsoft Excel, and then the size of the area was calculated with a formula in Excel. The results were defined as the pore size ($n = 100$).

2.6 | Mechanical property test

The cross-sectional area was measured with using a caliper, scaffold samples were cut into 5 mm \times 20 mm rectangular samples. The width and thickness of the samples were measured with calibrated digital calipers. Length was then measured as the clamp to clamp distance. The mechanical characteristics were tested with an Instron tensile testing machine (Model #5544, Instron Corp, Norwood, MA) equipped with a 100 N load cell. Tensile strength and elongation at break tests were conducted with a constant crosshead speed of 2 mm/min until failure.

2.7 | Actin filament staining

The myoblast specimens seeded on nanoyarn and non-woven nanofibrous scaffolds were rinsed twice with PBS (3 min per wash), and then the scaffolds were fixed with 4% paraformaldehyde for 10 min. Afterwards, the cells were penetrated using 5 μ L 0.1% Triton X and rhodamine-labeled phalloidin (Biotium, Fremont, CA) in 200 μ L PBS was used to stain the cytoskeletons, and DAPI (Beyotime, Haimen, Jiangsu, China) was used to stain the nuclei of the myoblasts on the scaffolds. The stained specimens were observed with a laser confocal microscope.

2.8 | Collagen type 1 immunofluorescence

At day 7, the cells seeded scaffolds were stained with immunofluorescence for collagen type 1 (ECM). The primary monoclonal antibodies were anti-collagen type 1 (Sigma, St. Louis, MO). After permeabilization with 0.2% Triton X-100 for 10 min at room temperature and incubation with the primary antibody for 60 min at 37°C, the specimens were washed with PBS three times and incubated with fluorescent labeled secondary antibody (Donkey anti-mouse IgG (H + L) Secondary Antibody, Alexa Fluor® 488) for 30 min at 37°C.

The nuclei were stained with DAPI for 5 min and rinsed three times. The specimens were examined with confocal fluorescence microscope.

2.9 | Urinary incontinence animal model creating and treatment

Thirty female rats (average body weight, 200 g) were divided into five groups. Rats in Group A undertook vaginal dilation (VD) only with a Foley catheter F12 (Bard, Kulim, Malaysia). The catheter was fixed to the skin at the orifice of vagina. Then 3 mL saline was injected into the catheter air sac to dilate the vagina. The catheter was loaded with a 250 g glass bottle at the end of catheter. Rats in Group B underwent VD and bilateral ovaries resection (BOR). The skin beside the spine was incised 2 cm along the spine. A 3-0 absorbable suture was used to ligature the oviducts, and the ovaries were resected. The wound was closed with 4-0 absorbable sutures. LPP were tested 8 weeks after the treatment. The model was created with LPP < 20 cmH₂O for later study.

Rats in Group C-E underwent non-cell sling surgery at the suburethra (C), cell-laden sling surgery at the suburethra (D), or were treated with tension-free vaginal tape-obturator (TVT-O)(E). Each group consisted of five female rats. The abdominal skin was incised 1 cm and the bladder neck was exposed. The sling was placed below the urethra on the bladder neck. All of the slings were fixed to the abdominal skin with 4-0 absorbable sutures and the skin was closed with the same sutures.

2.10 | Urodynamics

All of the animals in the study were anesthetized with urethane anesthesia (1.2 g/kg; ip). A polyethylene-50 catheter with a flared end was inserted through the bladder dome and the other end of the bladder catheter was connected to a microinfusion pump for continuous infusion of sterile PBS mixed with methylene blue at a rate of 0.1 mL/min in line with a pressure transducer (AD Instruments, Castle Hill, New South Wales, Australia) for intravesical pressure monitoring. The animals were then placed in the vertical position. When the first drop of blue liquid emerged at the outlet of the urethra, the LPP were set down. This procedure was performed three times and an average data were calculated.

2.11 | Histology evaluation

The sling specimens were rinsed with PBS and fixed in 4% paraformaldehyde for 15 min at room temperature followed by dehydration and paraffin embedding. Hematoxylin-eosin (H&E) and Masson's trichrome staining were performed to evaluate vascularization and collagen distribution, respectively.

2.12 | Statistical analysis

The quantitative data are presented as the mean \pm standard deviation. One-way analysis of variance was used to assess the statistical significance of results between each group. Difference was considered significant at $P < 0.05$.

3 | RESULTS

3.1 | Microstructure and mechanical properties of the nanoyarn slings

Figure 1 shows the SEM of the macro-structure of nanoyarn and nanofiber. The nanoyarn showed twisted fibers with large pores (Figures 1A and 1B). The ADSCs grew along the yarns (Figure 1C) and in the pores, which were surrounded by the yarns (Figure 1D). In the nanofiber scaffold, the pores were very small, and ADSCs only expanded on the surface of the scaffold. ADSCs were spread well on the nanofiber scaffold but exhibited random orientations (Figures 1G and 1H). The pore size in the nanoyarn scaffold ($32.5 \pm 3.32 \mu\text{m}^2$) was significantly larger than that of the nanofiber scaffold ($6.24 \pm 1.2 \mu\text{m}^2$) (Figure 1I). The nanoyarn porosity ($85.2 \pm 5.3\%$) significantly increased compared with that in the nanofiber scaffold ($72.3 \pm 9.4\%$) (Figure 1J).

Figures 1K and 1L displays the mechanical properties of the slings. The nanoyarn showed lower tensile strength (Figure 1J) but higher elongation at break (Figure 1K) compared with nanofiber scaffold and TVT-O. The tensile strength values among them were significantly different, elongation at break of the nanoyarn was significantly higher than the other slings, which indicated its high flexibility.

3.2 | Cells and sling morphology

Figure 2 shows the evaluation of ADSCs and the cell seeded scaffolds. The gross morphology of the cultured ADSCs exhibited a fibroblast-like spindle shape (Figure 2A) and showed the positive expression of vimentin, which is a biomarker of ADSCs (Figure 2E). In the H&E staining, the nanoyarn (Figure 2F) were found to yield an enhanced cell infiltration into the deep layer within 7 days of culturing of cells compared with that growing only on the surface of the nanofibrous scaffolds (Figure 2B). The ADSCs on the nanoyarn (Figure 2G) and nanofibrous scaffolds (Figure 2C) were stained with rhodamine-labeled phalloidin and DAPI. The ADSCs spread on the nanoyarn scaffold were visible with aligned actin filaments on day 7, which appeared to be the same morphology as muscle fibers compared to the filaments of ADSCs on nanofibrous scaffolds, which were randomly distributed. Figure 2H shows the immunofluorescence of collagen type 1 of ADSCs expression on the nanoyarn after 7 days of culture. ADSCs showed higher expression of

collagen type 1 on the nanoyarn, than that in nanofibrous scaffolds (Figure 2D).

3.3 | Animal model creating and evaluation

After 8 weeks, both groups were evaluated with urodynamic testing. The LPP of group A recovered to 38 cmH₂O (Figure 3A), but the group B kept the LPP to below 20 cmH₂O in 8 weeks (Figure 3B). The difference was significant ($P < 0.01$).

3.4 | Sling implantation and evaluation

The sling was placed below the urethra on the bladder neck. Then the end of the sling was fixed to the abdominal skin of the rat with 4-0 absorbable sutures. The immediate LPP post sling implantation was tested, and a value between 40 and 50 cmH₂O was the standard of tightness of the sling.

3.5 | Urodynamic follow-up post implantation

At 2, 4, and 8 weeks, the LPP of urodynamics was tested in each group of rats (Figure 4). A similar LPP was observed (~ 40 cmH₂O) from the immediate time point to the second week. After 2 weeks, the LPP varied among groups. In group C, which contained the rats with non-cell nanoyarn treatment, showed a decline of LPP with the time goes by ($P < 0.05$). In group D, rats undertaken cell-laden nanoyarn, maintained a similar LPP at the different time points. In group E, rats undertaken TVT-O treatment, kept LPP between 2 weeks and 4 weeks, however, at 8 weeks, the LPP showed a significant elevation compared to that at 2 weeks ($P < 0.01$).

3.6 | H&E and masson trichrome staining

The results of H&E are shown in Figure 5. In the non-cell nanoyarn, cells were located in the surrounding of the nanoyarn. In the middle of the non-cell nanoyarn, the naked nanofibers in nanoyarn were observed without cells and collagen distribution (Figures 5A and 5B). In the specimen of cell-laden nanoyarn, the cells infiltrated into majority of nanoyarn, and only a little part of naked nanoyarn could be found as shown by the black frame (Figures 5C and 5D). The sectioned specimens of the TVT-O sling had plastic debris, and multinucleated cells showing the inflammatory response with infiltrated the surrounding tissue (Figures 5E and 5F). There were no macrophages accumulated in the vicinity of the nanoyarn and nanofibers found on the H&E or Masson stained slides. Figure 5G shows the overall histology of cells seeded and the effects of nanoyarn on the bladder and urethra at 8 weeks. The nanoyarn was infiltrated with cells and integrated with the bladder neck to provide sufficient mechanical and biological support.

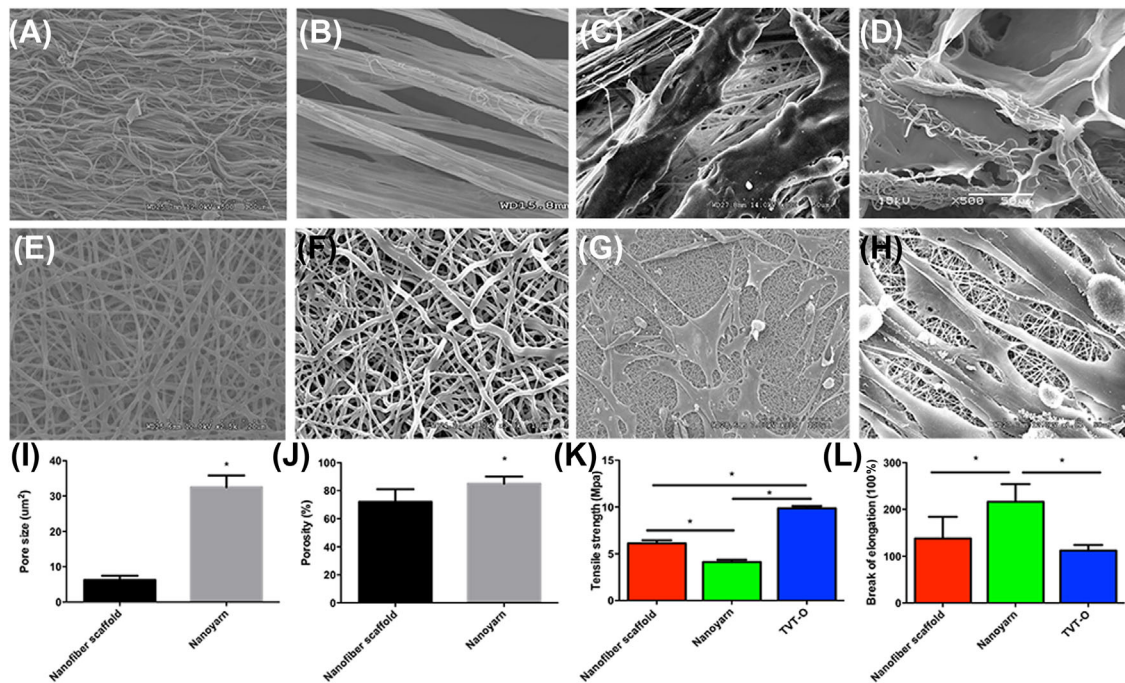


FIGURE 1 Scanning electron micrograph (SEM) of adipose-derived stem cells (ADSCs) on nanofiber scaffolds and nanoyarn. The twisted fibers in the nanoyarn aligned (A and B), but the nanofiber scaffold was random (E and F). ADSCs on nanoyarn (C and D) and nanofiber scaffolds (G and F). The pore size and (I) porosity (J) of the materials; The tensile strength (K) and break of elongation (L). Scale bars and length are labeled in each figure

The results of Masson's trichrome staining are shown in Figure 5 (blue, H–N). Only a small amount of collagen was observed around non-cell nanoyarn (Figures 5H and 5I). On the contrary, lots of collagen fibers formed and were distributed around cell-laden nanoyarn sites (Figures 5J and 5K). In addition, vessels with blood cells inside were

observed in the nanoyarn-filled region (Figures 5J and 5K). In the specimens of TVT-O sling, a substantial number of collagen fibers formed and was distributed around plastic debris of TVT-O (Figures 5L and 5M). Overall, at 8 weeks, plenty of collagen fibers had formed and were distributed around cell seeded nanoyarn surrounding the bladder neck,

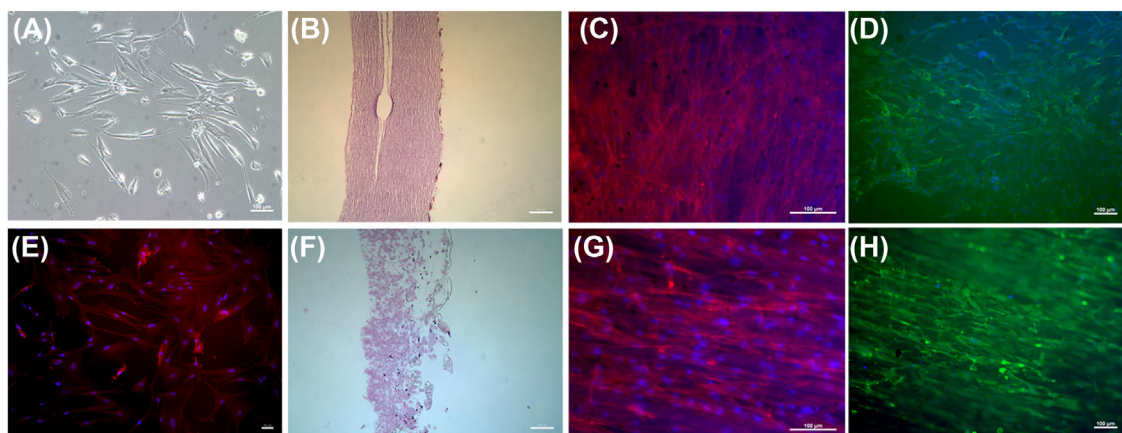


FIGURE 2 A, The gross morphology of adhering ADSCs in culture dish; B, The hematoxylin and eosin (H&E) staining of ADSCs on the surface of the nanofibers; C, The phalloidin and DAPI staining of ADSCs Actin filament and nuclei on nanofibers; D, Collagen type 1 of ADSCs on nanofibers; E, The immunofluorescence of vimentin of ADSCs; F, H&E staining of cell-laden nanoyarn after 7 days of culture; G, The phalloidin and DAPI staining of ADSCs Actin filament and nuclei on nanoyarn; H, The immunofluorescence of Collagen type 1 expressed by ADSCs on nanoyarn. Scale bars and their length are labeled in each figure

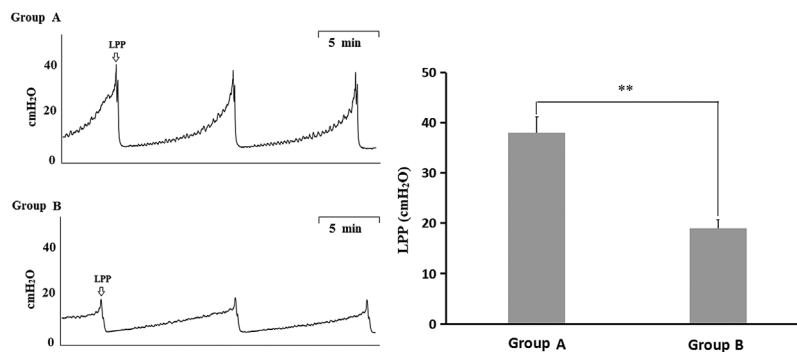


FIGURE 3 Group A, Female rats underwent dilation of the vagina; Group B, Rats underwent dilation of the vagina and ovary resection; Histogram showing the changes in urinary dynamics of leak point pressure (LPP) in different groups after 2 weeks. ** $P < 0.01$ indicates significant decreases in LPP (Group B vs Group A)

with thorough cell infiltration into the nanoyarn and abundant expression of extracellular matrix supporting the bladder neck (Figure 5N).

4 | DISCUSSION

Urinary incontinence is a common disease in urology and gynecology. Suburethral sling surgery has become a surgical choice for female patients.⁴ In clinic, slings can be classified according to their composition: autologous, heterologous and synthetic. However, a high recurrence rate exists, and commercial synthetic sling surgeries are often accompanied by several complications, such as urinary retention, erosions, extrusions, groin pain, leg pain, bladder perforation, urethral perforation, and deep vein thrombosis.^{9,10} Currently, with the rapid development of regenerative medicine, it might be a potential option to solve the underlying problem of UI patients.¹¹

Regenerative medicine in urology seeks to use a combination of cells and biomaterial to restore the natural continence mechanism. Although some progress in tissue-engineered sling has been gotten in the UI treatment, unfortunately, this approach has not been brought into the clinical setting. One of the most important reasons is the

limitation that the scaffold material with desirable properties for a sling is still under development.¹²

In the present study, the dynamic liquid electrospinning technique was applied to fabricate a P(LLA-CL)/collagen nanoyarn with numerous pores, highly aligned in a 3D micro-structure. In this process, the spinning speed and of the vortex and the structure of nanoyarn could be controlled by the volume of water in the upper container and the size of hole at the bottom of the container. The nanoyarn could mimic the native collagen morphologically and structurally. The characteristics of large pores, high porosity and aligned fibers provided a satisfactory biological environment for ADSCs. In our previous work, we evaluated the mechanical properties, the cell-material interaction, and genetic changing of the cells caused by this biomaterial. In this study, we introduced the material into an in vivo UI study to demonstrate its great potential as a urinary sling.

Stem cells are present in various adult and neonatal tissues. ADSCs are promising candidates for use in tissue engineering and regenerative medicine applications as they possess unique characteristics of self-renewal and differentiation into a variety of cell types.¹³ The LPP in the nanoyarn with seeded ADSCs was kept at nearly 40 cmH₂O, which demonstrated the efficacy of the stem cells. The mechanism

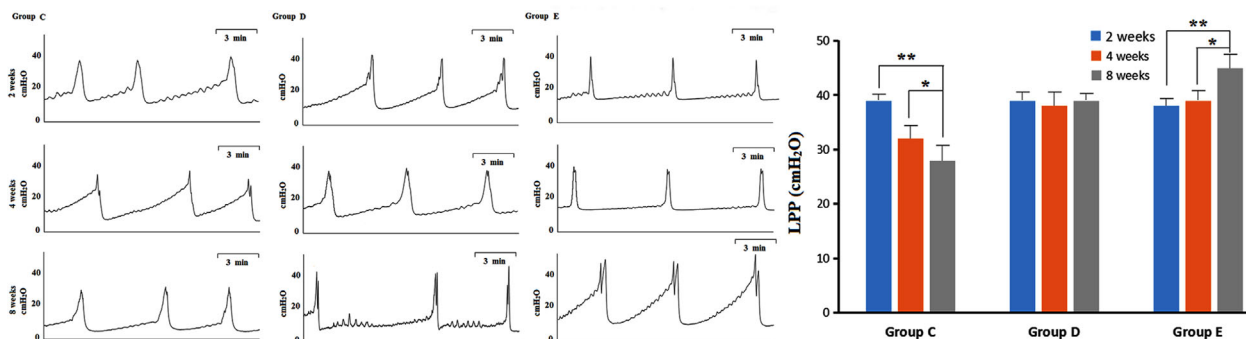


FIGURE 4 Urodynamic parameters of the nanoyarn (Group C), cell-laden nanoyarn (Group D), and TVT-O (Group E) at 2, 4, and 8 weeks. * $P < 0.05$, ** $P < 0.01$ indicate significant statistically difference at different time in leak point pressure (LPP) between Group C or Group E

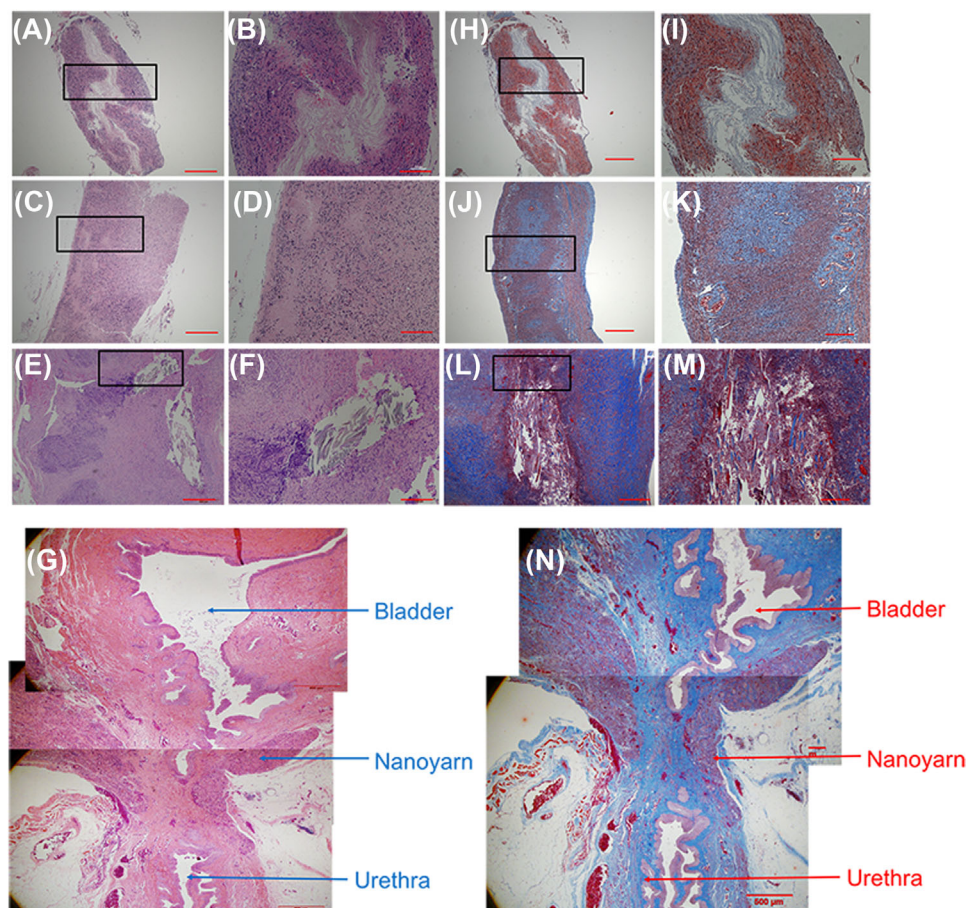


FIGURE 5 Hematoxylin and eosin (H&E) and Masson's staining of three kinds of slings. A, B, H, and I, non-cell nanoyarn; C, D, J, and K, cells-laden nanoyarn; E, F, L, and M, the TVT-O. G and N, The overall condition of the nanoyarn and bladder neck. Scale bar in A, C, H, J, E, G, L, N and B, D, I, K, F, M are 500 and 200 μm , respectively

should be deeply studied to clarify whether the function is paracrine-mediated or related to differentiation. Preclinical studies demonstrated that stem cells were able to differentiate into myoblasts and smooth muscle cells, which would reinforce the recovery of damaged bladder sphincter. Furthermore, a paracrine mechanism of stem cells has been reported because of secretion of growth factors, exosomes and miRNAs that modulate local inflammatory responses to damage. Perhaps, that's why the cell-laden nanoyarn showed deeper cell infiltration and fewer multinucleated cells compared to the non-cell nanoyarn and TVT-O. The ADSCs are liable to proliferate on the nanoyarn, which is an advantage of the material compared to a commercial sling. In the cell-laden nanoyarn 8 weeks post implantation, several vessels could be found in the edges of the material, which indicated the benefit of the angiogenic function of ADSCs and the porous structure of the nanoyarn.

Modifying sling properties using tissue engineering seems promising. Various natural or synthetic polymers have been fabricated into engineered scaffolds using the electrospinning method to repair many different types of tissues.¹⁴ Ideal engineered scaffolds should mimic the native

ECM to support cell adhesion, proliferation and differentiation, thereby facilitating tissue formation. Electrospinning is reported to be an efficient and economical process to fabricate scaffolds for tissue engineering applications. One of the advantages of electrospun fibers is the high surface-to-volume ratio which is extremely suitable for cell growth.¹⁵ Promising as electrospinning technique is, the fabrication of scaffolds with controlled 3D property remains a problem, due to its nature of layer by layer deposition pattern of the nanofibers. To solve this problem, previous methods have included salt leaching, ice crystal formation, sacrificial fibers or increasing the fiber diameter.^{14,16} However, these methods decreased the mechanical strength and inhibited the cell growth.

Different methods have been used to create UI model in lab animals, such as bilateral pudendal nerve transection or VD. In our study, we found that a prolonged UI effect could not be obtained with only VD, and BOR was necessary to maintain the UI condition. SUI is the most common type of incontinence in female population, however, various animal models could not mimic this condition. On the other hand, the most realistic animal model should be a primate, but ethical

problems prevent their use. In our study, we creatively combined two methods to create and maintain the condition of low LPP, which provided a method for future studies. More robust experiments will be performed in a large animal model in the future.

5 | CONCLUSION

The treatment of urinary incontinence is a difficulty in urology, and the current commercial biomaterials could not meet the need of biological sphincter repair. In this study, we found that ASDCS and nanoyarn could be combined cooperatively when implanted at the suburethra to treat the urinary incontinence. The nanoyarn and ADSCs maintained LPP of the bladder and enhanced the collagen deposition and muscular tissue formation. In conclusion, cell-laden nanoyarn could be a promising tissue engineered biomaterial for urinary incontinence treatment.


ACKNOWLEDGMENTS

It is very much appreciated that the contribution has been made by the Biomaterials and Tissue Engineering Laboratory, College of Chemistry & Chemical Engineering and Biotechnology, Donghua University in the work of fabrication of scaffold. It is also very much appreciated that Wake Forest Institute for regenerative medicine, Winston-Salem, North Carolina, USA made a lot of contributions to this study. The study was supported by Science and Technology Commission of Shanghai Municipality (14JC1492100). The animals used in this study were proved by the ethical committee of shanghai sixth people's hospital (No: 2017-0240).

CONFLICT OF INTEREST

None declared.

ORCID

Nailong Cao  <http://orcid.org/0000-0001-9328-6543>

REFERENCES

- Norton P, Brubaker L. Urinary incontinence in women. *Lancet*. 2006;367:57–67.
- Anding R, Schoen M, Kirschner-Hermanns R, Fisang C, Müller SC, Latz S. Minimally invasive treatment of female stress urinary incontinence with the adjustable single-incision sling system (AJUST) in an elderly and overweight population. *Int Braz J Urol*. 2017;43:280–288.
- Chapple CR, Osman NI, Mangera A, et al. Application of tissue engineering to pelvic organ prolapse and stress urinary incontinence. *Low Urin Tract Symptoms*. 2015;7:63–70.
- Kim MY, Choi SD, Ryu A. Is complementary and alternative therapy effective for women in the climacteric period? *J Menopausal Med*. 2015;21:28–35.
- Zheng Y, Roberts MA. Tissue engineering: scalable vascularized implants. *Nat Mater*. 2016;15:597–599.
- Wu J, Huang C, Liu W, et al. Cell infiltration and vascularization in porous nanoyarn scaffolds prepared by dynamic liquid electrospinning. *J Biomed Nanotechnol*. 2014;10:603–614.
- Zhang K, Guo X, Li Y, et al. Electrospun nanoyarn seeded with myoblasts induced from placental stem cells for the application of stress urinary incontinence sling: an in vitro study. *Colloids Surf B Biointerfaces*. 2016;144:21–32.
- Fu Q, Song XF, Liao GL, Deng CL, Cui L. Myoblasts differentiated from adipose-derived stem cells to treat stress urinary incontinence. *Urology*. 2010;75:718–723.
- Borazjani A, Pizarro-Berdichevsky J, Li J, Goldman HB. Surgeons' views on sling tensioning during surgery for female stress urinary incontinence. *Int Urogynecol J*. 2017.
- Szell N, Komisaruk B, Goldstein SW, Qu XH, Shaw M, Goldstein IA. Meta-analysis detailing overall sexual function and orgasmic function in women undergoing midurethral sling surgery for stress incontinence. *Sex Med*. 2017;5:84–93.
- Kajbafzadeh AM, Mozafarpour S, Ladi Seyedian SS, Khorramirouz R, Nasser Hojjati H. Decellularized dermal strip as a suburethral sling in a rat model of stress urinary incontinence. *Int Urol Nephrol*. 2015;47:1303–1310.
- Hakim L, De Ridder D, Van der Aa F. Slings for urinary incontinence and the application of cell-based therapy. *Adv Drug Deliv Rev*. 2015; 82–83:22–30.
- Zhang XM, Zhang YJ, Wang W, Wei YQ, Deng H. Stem cell treatment in crohn's disease. *Hum Gene Ther*. 2017.
- Lee JM, Chae T, Sheikh FA, et al. Three dimensional poly(epsilon-caprolactone) and silk fibroin nanocomposite fibrous matrix for artificial dermis. *Mater Sci Eng C Mater Biol Appl*. 2016;68: 758–767.
- Cha SH, Lee HJ, Koh WG. Study of myoblast differentiation using multi-dimensional scaffolds consisting of nano and micropatterns. *Biomater Res*. 2017;21:1–9.
- Park YR, Ju HW, Lee JM, et al. Three-dimensional electrospun silk-fibroin nanofiber for skin tissue engineering. *Int J Biol Macromol*. 2016;93:1567–1574.

How to cite this article: Zhang K, Cao N, Guo X, et al. The fabrication of 3D surface scaffold of collagen/poly (L-lactide-co-caprolactone) with dynamic liquid system and its application in urinary incontinence treatment as a tissue engineered sub-urethral sling: In vitro and in vivo study. *Neuourology and Urodynamics*. 2018;37:978–985. <https://doi.org/10.1002/nau.23438>